CAV2021
11th International Symposium on Cavitation
May 10-13, 2021, Daejon, Korea

Kelvin-Helmholz Instability Driven Shedding of Cavitation Clouds in Microchannels

Darjan Podbevšek[1], Martin Petkovšek[1], Claus Dieter Ohl[2], Matevž Dular[1]*
[1]Faculty of Mechanical Engineering, University of Ljubljana, Askerceva 6, 1000 Ljubljana, SI-Slovenia
[2]Institute for Physics, Otto von Guerricke University, Universitätsplatz 2, 39106 Magdeburg, DE-Germany

Abstract: The paper shows visualization of cavitation inside a microchannel. While the initial aim of the study was to establish supercavitating conditions inside a microchannel, yet we found that this regime is suppressed due to the formation of a Kelvin-Helmholtz instability, which triggers a semi periodical attached cavity collapse. In-depth observations using high speed imaging with visible light and X-rays revealed that this is in fact besides the re-entrant jet and the shock wave a third mechanism leading to the shedding of cloud cavitation.

Keywords: Cavitation, Kelvin-Helmholtz instability, Microchannel

1. Introduction

It is known that cavitation behavior and its dynamics may change when scaling down the flow tract (Mishra & Peles 2005). At larger scales (order of centimeters) one of the most distinctive characteristics of developed cavitation is the process of cavitation cloud shedding. Detailed studies by Dular et al. (2005, 2007); Ganesh et al. (2016, 2017); Laberteaux & Ceccio (2001a, 2001b) helped to reveal two mechanisms that govern the shedding process: the re-entrant jet and the shock wave.

With decreasing the size, the viscous forces start to become relevant as the Reynolds number drops. It was shown for example by Dular et al. (2012) that at a scale of several millimeters and below the re-entrant jet cannot fully develop – mainly due to a relatively larger bubbles compared to the size of the flow tract. As a result, the cavitation cloud shedding process ceases its periodic behavior and becomes chaotic.

By further reducing the size of the channels, i.e. to microfluidics new properties of the flow at the submillimeter scale are revealed. Here, microfluidics offers the possibility of using minute quantities of precious or toxic fluids (Ayela et al. 2013; Kim et al. 2017; Podbevsek et al. 2018; Stieger et al. 2017). As the Reynolds number drops the viscous and surface tension forces start to affect the dynamics of the vapor bubbles. Scaling down to microchannels reveals unique properties of the flow, such as liquid metastability, the two-phase flow hysteresis and discrepancies in inception and desinent cavitation number (Medrano et al. 2012; Mishra & Peles 2005). These are mostly consequences from the reduction of free stream nuclei and a lack of nucleation on channel walls.

Understanding the cavitation dynamics on a submillimeter scale is of a crucial importance for applications in the automotive industry. In fuel injection systems, the fuel is sprayed into the cylinder through a nozzle with a diameter of much smaller than a millimeter. While cavitation is always present, on one hand its appearance is desirable, as is promotes atomization of the fuel, leading to more efficient combustion, but on the other hand it causes erosion to the nozzle. An in-depth understanding of cavitation dynamics on these small scales is therefore essential for optimization. The second application is water treatment, where cavitation and its effects are used to destruct bacteria or inactivate viruses. For such application it is sometimes essential to establish supercavitating conditions in relatively compact channels. Thus, an understanding of small scale instabilities in such geometries is of crucial importance.

* Corresponding Author: Matevz Dular, matevz.dular@fs.uni-lj.si

2. Materials and Methods

Experiments were performed at University of Ljubljana (Slovenia), Otto von Guericke University Magdeburg (Germany) and at Argonne National Laboratory – Advance photon source (USA). In all locations the same experimental setup was used.

The experimental set-up is shown in Fig.1. Microchannels are made of 450μm thick stainless-steel sheets that include a laser cut convergent-divergent constriction by sandwiching them between two acrylic glass plates of 10mm thickness, see Fig.1 (right, test section side view). The convergent-divergent (18°- 10°) constriction has a throat height of 675 μm.

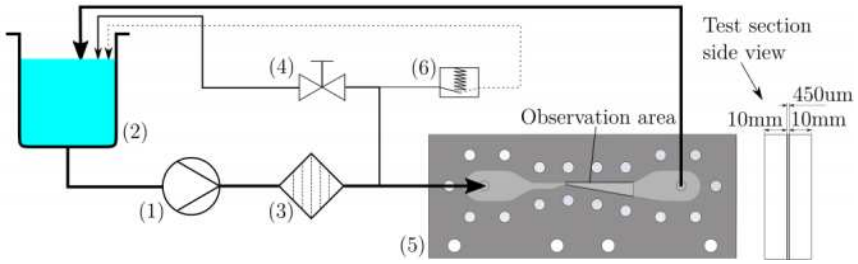

Figure 1. Experimental set-up.

A small gear pump (1) transports liquid from the reservoir (2) through the 10μm nylon and 1μm glass fiber filter (3). The back-pressure regulator (4) limits the flow on the primary line of the setup, therefore setting the upstream pressure in the microchannel (5). A safety relief valve (6) is installed in the system to prevent over-pressurization in case of clogging or user error. The flow from the channel and the two valves is then gathered back to the reservoir.

Images were captured by either CMOS high speed cameras (Photron SA-Z and Photron Mini AX200) at a framerate of typically 200,000 fps. A modellocked fiber based femtosecond laser (EXPLA FemtoLux 3, 515nm wavelength) was used for backlite illumination. Approximately 200 fs long laser pulses were synchronized with the image acquisition such that a single laser pulse illuminated each frame. In addition high speed X-ray visualization was performed at the Argonne National Laboratory – Advance photon source with a Photron SA-Z high-speed camera, which recorded the image projected onto a scintillator screen. The phase contrast imaging technique, explained in detail in (Khlifa et al. 2017), allows for imaging throughout the depth of the channel, revealing details that would be unseen or likely misinterpreted in classical backlight high-speed imaging.

3. Results

Figure 2 shows typical images of the Kelvin-Helmholtz instability occurrence in two different microchannels. The flow is from the left to the right.

The selected images do not belong to the same sequence and are shown only as a representation of the cavitation structure topology in the channel. We can obviously observe the rise of the interface and subsequent the roll-up of the waves that eventually leads into collapse of the supercavitating structure.
Similar to our previous study of cavitation in milichannels (Petkovšek et al. 2020) we find that cavitation resembles the condition of supercavitation. But in contrast to its macroscopic manifestation the one in the microchannel is not stable. Its size oscillates periodically to large extent and small cavitation structures are

* Corresponding Author: Matevz Dular, matevz.dular@fs.uni-lj.si

shed from its closure. A second difference from the larger scales (Petkovšek et al. 2020) is that no shock waves are observed, that should be clearly visible with the particular illumination. Instead, the interface between the quasi supercavitating bubble and the liquid jet is wavy and oscillating. We identify this shape as a result of the Kelvin Helmholz instability. It will be shown later that this instability is not only causing the oscillation of the attached cavity but also results in the shedding of cavitation clouds.

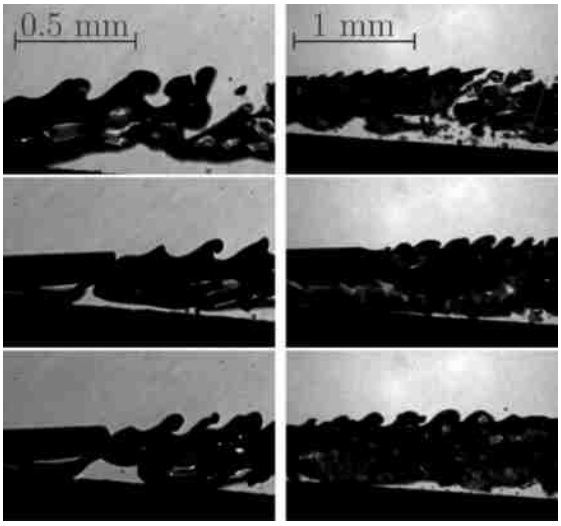

Figure 2. Examples of Kelvin-Helmholtz instability occurrence in Venturi microchannel.

Overall, four distinctive phenomena, which are not present in developed cavitating flow in channels with larger dimensions, could be determined. Namely i) formation of a single stable cavitation bubble, ii) shedding of predominantly small cavities, iii) formation of Kelvin-Helmholtz instability and iv) the absence of shock waves.

Particularly interesting is the onset of the Kelvin-Helmholtz instability and its contribution to the dynamics of cavitation structure shedding process. Figure 3 shows a typical cycle of the attached cavity oscillation.

From the observation of the entire flow field (Fig. 3) it is obvious that the process of destabilization of the attached cavitation pocket is initiated at the cavity closure line. The attached cavity firstly grows. In the first image one can see the fully extended attached supercavitating bubble. Due to the divergent angle of the Venturi the flow velocity decreases, and the pressure increases to a value at which further growth is limited. At the cavity closure line the re-entrant jet builds up (frame 2). As the growth of the cavity stagnates, significant shear flow forms between the vapour and the liquid at the interface. The rear part of the cavity begins to oscillate mildly that affects the pressure balance. A decreased gap between the interface and the upper channel wall forces the liquid jet to accelerate, what induces a local drop in the pressure above the interface. A newly established pressure difference pushes the interface further and the disturbance grows. At the same time the shear flow stretches the interface and by this builds a vortex - the Kevin-Helmholtz instability forms. As the interface curls up, it becomes unstable and eventually breaks up, shedding multiple small vaporous cavities (possibly single bubbles) downstream (frames 3 to 5). The new cavity closure line moves upstream and the process is continued until a low-pressure region, closer to the throat of the Venturi is reached (frame 6). At this point the cavitation pocket is somewhat stabilized and begins to grow at a slightly slower pace than the velocity of the liquid jet. As a result, the shear flow, although smaller, is still present - cavity shedding due to the presence of the Kelvin-Helmholtz instability

* Corresponding Author: Matevz Dular, matevz.dular@fs.uni-lj.si

continues (frames 7 to 11). The cavity growth accelerates and reaches the same velocity as the liquid jet. Hence, the shear flow is minimized, the cavity interface becomes stable, and the shedding briefly ceases before the cycle is repeated.

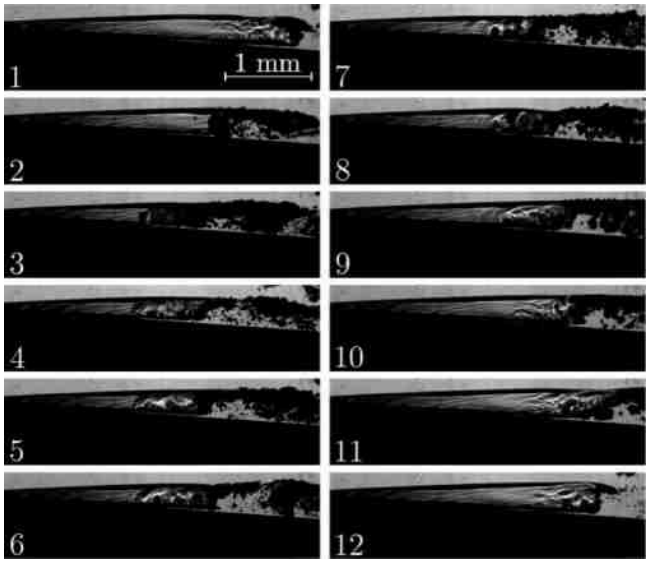

Figure 3. A sequence showing one cycle of a typical shedding period. The time difference between two images is 0.1ms. In images No.2, 3, 8, 9 and 10 one can observe the occurrence of Kelvin-Helmholtz instability.

A more detailed look into the unstable interface can be obtained from the high speed recording using the X-Ray absorbance. This phase-contrast enhancement technique provided by the APS (Advanced Photon Source) synchrotron beam is presented in Figure 4.

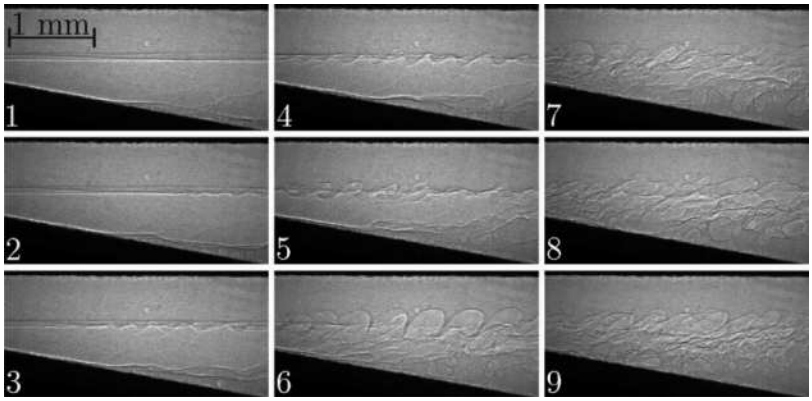

Figure 4. A sequence taken during an experimental campaign by fast x-ray imaging in a 675x450 μm Venturi channel. The time difference between two images is 0.1 ms. One can clearly observe the occurrence of Kelvin-Helmholtz instability.

The first frame depicts a smooth interface between the liquid jet and the vapour phase. Close to the channel wall (frame 1 and 2) one can see a thin liquid layer which slowly moves upstream. This is a result of a separation of the supercavitating structure from the wall and the very weak classical re-entrant jet. The stagnation of the cavity growth results again in a shear flow at the interface and the Kelvin-Helmholtz

* Corresponding Author: Matevz Dular, matevz.dular@fs.uni-lj.si

instability builds up, firstly at the cavity closure before it moves upstream (frames 2 to 4). At the same time the attached cavity still remains purely vaporous (supercavity). In frame 5 one can observe the beginning of the rollup, which becomes more pronounced in frame 6. Finally, as a result of Kelvin-Helmholtz instability, we witness the breakup of the attached supercavity in frames 7 to 9.

The phenomenon likely also occurs in larger geometries, but does not develop fully, due to very small changes in shear velocities at the interface. This is further discussed in the following section.

4. Conclusions

There are some mentions that Kelvin-Helmholz instabilities could exist in cavitating flow in microchannels, but this has not been investigated thoroughly. Here we show detailed observations of Kelvin-Helmholz instabilities, but more importantly we find that its occurrence destabilizes supercavitation in microchannels. This is due to the uniquely confined flow, which triggers the Kelvin-Helmholtz instability from the cavity closure line. The flows were investigated by high speed image capturing with visible light and X-rays. The recordings reveal how the instability forms, grows and eventually triggers the shedding of relatively small cavities. The second result of the study is that no shock waves were observed upon collapse of the shedded bubbles downstream.

Acknowledgments: The authors acknowledge the financial support from the European Research Council (ERC) under the European Union's Framework Program for research and innovation, Horizon 2020 (grant agreement n 771567 – CABUM) and the Slovenian Research Agency (Core funding No. P2-0401and project No. J7-1814). Use of the Advanced Photon Source at the Argonne National Laboratory was supported by the US Department of Energy, Office of Science, Office of Basic Energy Sciences. Finally, M. Dular acknowledges the support from the Humboldt Foundation Friedrich Wilhelm Bessel Research Award.

References

Ayela, F., Medrano-Muñoz, M., Amans, D., … Ledoux, G. (2013). Experimental evidence of temperature gradients in cavitating microflows seeded with thermosensitive nanoprobes. Physical Review E, 88(4), 043016-(1-5).

Dular, M., Bachert, R., Schaad, C., & Stoffel, B. (2007). Investigation of a re-entrant jet reflection at an inclined cavity closure line. European Journal of Mechanics B/Fluids, 26, 688–705.

Dular, M., Bachert, R., Stoffel, B., & Širok, B. (2005). Experimental evaluation of numerical simulation of cavitating flow around hydrofoil. European Journal of Mechanics B/Fluids, 24, 522–538.

Dular, M., Khlifa, I., Fuzier, S., Adama Maiga, M., & Coutier-Delgosha, O. (2012). Scale effect on unsteady cloud cavitation. Experiments in Fluids, 53(5), 1233–1250.

Ganesh, H., Mäkiharju, S. A., & Ceccio, S. L. (2016). Bubbly shock propagation as a mechanism for sheet-to-cloud transition of partial cavities. J. Fluid Mech, 802, 37–78.

Ganesh, H., Mäkiharju, S. A., & Ceccio, S. L. (2017). Bubbly shock propagation as a mechanism of shedding in separated cavitating flows. Journal of Hydrodynamics, 29(6), 907–916.

Khlifa, I., Vabre, A., Hočevar, M., … Coutier-Delgosha, O. (2017). Fast X-ray imaging of cavitating flows. Experiments in Fluids, 58(11), 157.

* Corresponding Author: Matevz Dular, matevz.dular@fs.uni-lj.si

Kim, J., Michelin, S., Hilbers, M., … Gacoin, T. (2017). Monitoring the orientation of rare-earth-doped nanorods for flow shear tomography. Nature Nanotechnology, 12(9), 914–919.

Laberteaux, K. R., & Ceccio, S. L. (2001a). Partial cavity flows. Part 1. Cavities forming on models without spanwise variation. Journal of Fluid Mechanics, 431, 1–41.

Laberteaux, K. R., & Ceccio, S. L. (2001b). Partial cavity flows. Part 2. Cavities forming on test objects with spanwise variation. Journal of Fluid Mechanics, 431, 43–63.

Medrano, M., Pellone, C., Zermatten, P. J., & Ayela, F. (2012). Hydrodynamic cavitation in microsystems. II. Simulations and optical observations. Physics of Fluids, 24(4), 047101.

Mishra, C., & Peles, Y. (2005). Cavitation in flow through a micro-orifice inside a silicon microchannel. Physics of Fluids, American Institute of Physics Inc. doi:10.1063/1.1827602

Petkovšek, M., Hočevar, M., & Dular, M. (2020). Visualization and measurements of shock waves in cavitating flow. Experimental Thermal and Fluid Science, 119, 110215.

Podbevsek, D., Colombet, D., Ledoux, G., & Ayela, F. (2018). Observation of chemiluminescence induced by hydrodynamic cavitation in microchannels. Ultrasonics Sonochemistry, 43, 175–183.

Stieger, T., Agha, H., Schoen, M., Mazza, M. G., & Sengupta, A. (2017). Hydrodynamic cavitation in Stokes flow of anisotropic fluids. Nature Communications, 8(1), 15550.

* Corresponding Author: Matevz Dular, matevz.dular@fs.uni-lj.si